



MODELING SYSTEM OF A FLEXIBLE STRUCTURE WITH HYDRAULIC ACTUATION USING BOND-GRAPHS

Euler Gonçalves Barbosa

IAE/CTA - Instituto de Aeronáutica e Espaço, euler@mec.ita.cta.br
São José dos Campos - SP - CEP: 12228-900

Luiz Carlos Sandoval Góes

Departamento de Projetos, Divisão de Engenharia Mecânica-Aeronáutica
ITA/CTA - goes@mec.ita.cta.br
São José dos Campos - SP - CEP: 12228-900

***Abstract.** This paper presents the modeling and control system of a flexible structure (plate) subjected to a torque generated by hydraulic rotatory actuator controlled by an electro hydraulic servo valve. The flexible structure consists of a plate fixed to a center post, which is supported on a semi hemispherical gas-bearing table and is positioned to a desired angle by the hydraulic motor. The actuating torque excites various natural vibration modes on longitudinal and transversal directions allowing the coupling of several dynamic effects between the hydraulic actuation system and the flexible plant. An analog servo-controller develops a control torque that may be used to move the structure and minimize the amplitudes of the vibration. In this paper we use the Hamilton's Principle to derive the equations of motion of the slewing flexible plate coupled to the dynamics of the servo-hydraulic system loaded by the central hub. The assumed modes method is applied to discretize the dynamic system, using well-known shape functions of an Euler-Bernoulli beam in two directions. The resulting equations are presented in a unified Bond Graph language, resulting a unique model for the flexible structure and hydraulic actuation system, which is shown to be useful to control the system.*

Keywords: Modeling, Plates, Control, Mathematical Modeling, Bond Graphs

1. INTRODUCTION

The modeling process in control systems, is a loop of basic steps involving modeling, controller design and controller validation. The system modeling is the first phase and its not an easy task principally if involves multidisciplinary systems. The Bond Graph graphical language (BG) can be applied with great advantage to the modeling of complex dynamic systems with many intervening energy domains. This kind of dynamic system modeling is particularly interesting for the development of analog or digital control projects of mechatronic systems. The advantages of the method are related to the unified representation of different energy domains, and the simplified manner of representing complex dynamic effects, for all type of physical systems. Changes on projects or retrofiting can be made with few changes in the BG model. So in this sense, time and effort can be minimized, resulting in a system design methodology compatible with the principles of the Mechatronic Engineering, which is system functional optimization with minimal spent of energy. This work focuses the dynamic BG modeling and identification of a hydraulic plant controlling the slew motion of a flexible plate, which can be considered representative of many practical problems in airborne satellites, aeronautical and naval structures, as well as in automobilist systems and air conditioner products. The experimentally assembled system was used to test the

adequacy of the BG model to represent the behavior of the hydraulic and flexible plant, by comparing analytical derived transfer functions with the experimental ones. A BG model is proposed by considering the details of the hydraulic and flexible plate separately, and finally combining the effects to reach a BG that represents the full system. The State-space model of the system is derived using the software CAMP-G.

2. SYSTEM DESCRIPTION

Figure (1) shows the experimental assembly of the flexible plate mounted on a semi-hemispherical gas bearing table, and its rigid supporting structure manufactured at ITA/CTA.

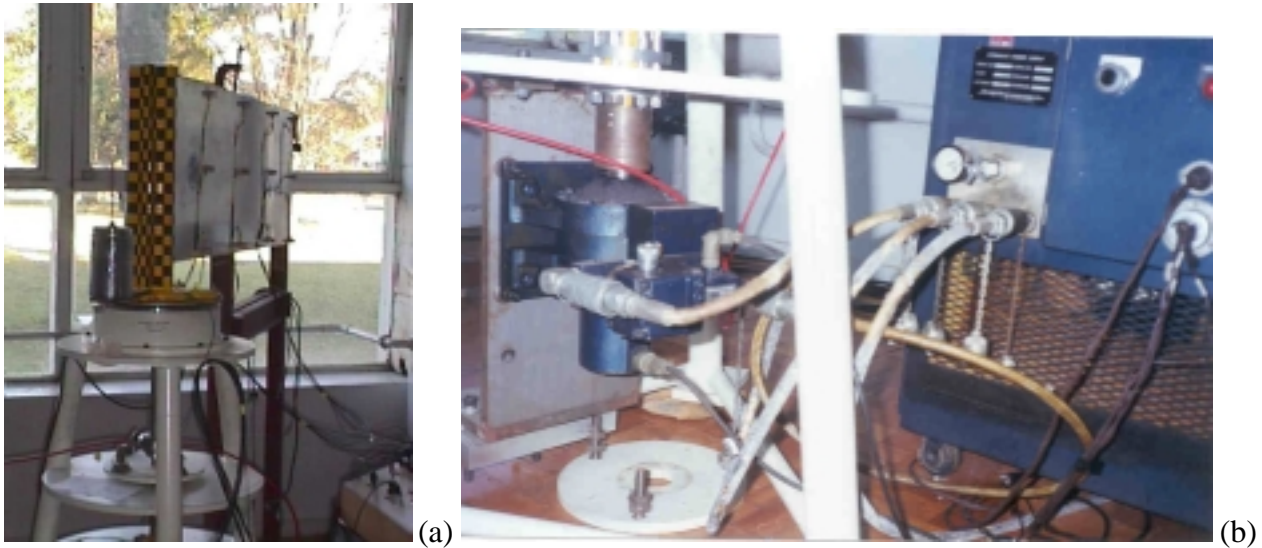


Figure 1. (a) View of the flexible structure experiment and supporting gas-bearing table; (b) Detail of the electro hydraulic servo valve and rotary servo hydraulic actuator

2.1 The hydraulic plant and Bond Graph Model

The hydraulic plant consists of a pressure supply unit, an electro-hydraulic servo valve and a rotary hydraulic actuator (vane motor). The output axis of the vane motor is coupled to a torsion bar that drives the central hub. The hub is supported by a gas bearing system, and is attached to the flexible plate by a central post. A feedback position control system is used to control the slewing motion of the flexible appendage. Fig. (1b) shows the details of the hydraulic plant that generates the control torque actuating on hub, through the torsion shaft.

The electronic control circuit consists of linear power operational amplifier driven by an error detector amplifier. The feedback signal is obtained from a potentiometer at the actuator axis, $y_{pot}(t)$. The power amplifier signal, $e_{in}(t)$, is fed to the torque motor of a four-way, two-stage electro-hydraulic servo valve. The servo valve spool position, $x_v(t)$, is controlled by the pressure difference across the spool, $p_c(t) - p_3(t)$, generated by the motion of a flapper-nozzle valve, $x_f(t)$. The flapper motion is controlled by the displacement of the linear voice-coil actuator. The spool position controls the line pressure ($p_1 - p_2$) of the rotary actuator. A schematic view of the electro-hydraulic servo actuator system is shown in Fig. (2a).

The Bond-Graph model of the servo actuator is shown in Fig. (2b). Here, BG1 is the BG fragment of the voice coil actuator and flapper-nozzle control valve. The motor coil is modeled by a resistor, R_{bob} , in series with the coil inductance, L_{bob} . The coil current is transformed in a linear control force through a gyrator effect with transformation constant, k_ϕ . The flapper dynamics is modeled by an inertia, m_f , a viscous friction, b_f , and a spring, k_f . The flow variable indicated in the BG1 fragment is the flapper velocity, v_f .

The feedback control system with the LOES in the direct path is described the following state space equations:

$$\begin{bmatrix} \dot{\theta}_a \\ \dot{p}_6 \\ \dot{q}_3 \end{bmatrix} = \begin{bmatrix} 0 & \frac{1}{I_6} & 0 \\ 0 & 0 & \frac{D_m}{C_3} \\ -k_{sv} A_1 A_2 k_{POT} & -\frac{D_m}{I_6} & -\frac{1}{R_7 C_3} \end{bmatrix} \begin{bmatrix} \theta_a \\ p_6 \\ q_3 \end{bmatrix} + \begin{bmatrix} 0 \\ 0 \\ k_{sv} A_1 A_2 \end{bmatrix} . r \quad y_{POT} = \begin{bmatrix} k_{POT} & 0 & 0 \end{bmatrix} \begin{bmatrix} \theta_a \\ p_6 \\ q_3 \end{bmatrix} \quad (1.a,b)$$

The dynamic model derived above was used to interpret the experimental observations of the hydraulic system transfer function. The experimental results are shown in Fig. (4a) and Fig. (4b), which show the magnitude and phase of the closed-loop transfer function, respectively. The experimentally identified transfer function in the direct path of the closed loop system can be described by the following parametric description estimated by standard least-square technique,

$$G_{PH\ est}(s) = \frac{2250000}{s(s+65)(s+753)} \quad (2)$$

Figure (4a) and Fig. (4b) also show the comparison between the estimated (green) and the experimentally determined (blue) closed-loop hydraulic system frequency response function.

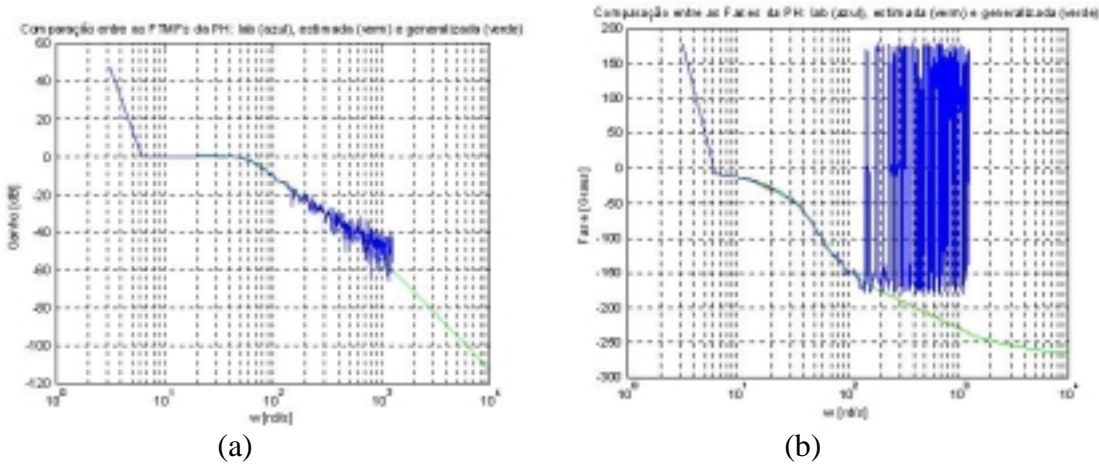


Figure 4. (a) Gain versus frequency, experimental transfer function (blue), LOES (green);
(b) Phase versus frequency, experimental transfer function (blue), LOES (green)

From the above-identified frequency response functions one can estimate the physical parameters of the proposed LOES model for the hydraulic actuation system. The dynamic parameters are $C_3 = 5,28 \cdot 10^{-11}$ [m⁵/N], $I_6 = 0,0025$ [kg.m²] and $R_7 = 3,8 \cdot 10^7$ [N.s/m⁵]. We point out that the experimental identification of the hydraulic plant was realized with the motor uncoupled to the torsion shaft.

2.2 The Flexible Plant

The flexible appendage consists of a thin rectangular plate made of aluminum foil, with the following physical parameters:

Young's modulus,	$E = 6,89 \cdot 10^{10}$ [N/m]	Mass density, $\rho = 2795$ [kg/m ³]
Length,	$a = 1,41$ [m]	Weight, $b = 46,85$ [cm]
Plate thickness,	$h = 2,65$ [mm]	

The vibrations of the flexible plate are measured with 12 piezoelectric accelerometers uniformly distributed over the surface of the plate, as shown in the detail of Fig. (5a).

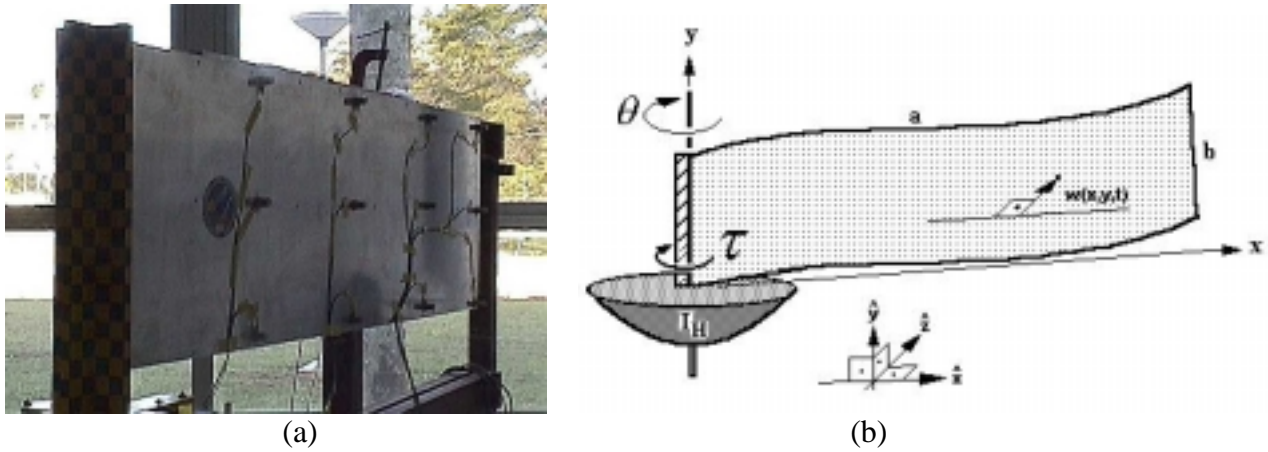


Figure 5. (a) View of the instrumented flexible plate; (b) Schematic view and central hub

3. DYNAMIC MODEL OF THE FLEXIBLE APPENDAGE

The flexible plate is fixed to a central inertia, which is supported on a gas bearing system, as depicted in the schematic view shown in Fig. (8b). The figure also shows the reference systems, and the main parameters used in the description.

The plate has a thickness of $h = 2,65$ [mm], which is much smaller than its length $a = 1,41$ [m], and width $b = 46$ [cm], and for this reason we consider the thin plate theory with the standard Kirchhoff's assumptions. To get the governing equations of motion of the plate and hub, we use the Hamilton's Principle:

$$\delta \int_{t_0}^{t_f} (K - V_{int} + W_{nc}) dt = 0 \quad (3)$$

where the kinetic energy is:
$$K = \frac{1}{2} I_H \dot{\theta}^2 + \frac{1}{2} \int_0^a \int_0^b m (x\dot{\theta} + \dot{w})^2 dx dy \quad (4)$$

with “ m ” the mass per unit area. The plate strain energy is computed by:

$$V_{int} = \frac{1}{2} \int_0^a \int_0^b D \left\{ \left(\frac{\partial^2 w}{\partial x^2} + \frac{\partial^2 w}{\partial y^2} \right)^2 - 2(1-\nu) \left[\frac{\partial^2 w}{\partial x^2} \frac{\partial^2 w}{\partial y^2} - \left(\frac{\partial^2 w}{\partial x \partial y} \right)^2 \right] \right\} dx dy \quad (5)$$

and the work realized by the torque “ τ ” applied to the hub is $W_{nc} = \tau \theta$.

Applying the Lagrangean formalism one arrives at the following result for the dynamics of the slewing plate, with the change of variables: $z(x, y, t) = w(x, y, t) + x\theta$:

$$\begin{cases} I \ddot{\theta} + \int_0^a \int_0^b m x \frac{\partial^2 z}{\partial t^2} dx dy = \tau \\ D \nabla^4 z + m \frac{\partial^2 z}{\partial t^2} = 0 \end{cases} \quad (6.a,b)$$

where $I = I_H + 2I_p$, with I_H the mass moment of inertia of the hub (3,5[kg.m²]), and I_p the area moment of inertia of the plate about the y axis, $I_p = \int_0^b \int_0^a m x^2 dx dy$.

The distributed parameter system described by Eq. (6a,b) can be simplified by considering the vibrations around a desired angular position, and taking an approximate solution to the flexible displacements of the plate in terms of admissible functions expressed by the series:

$$z(x, y, t) = \sum_{n=1}^R \sum_{m=1}^S \phi_{nx}(x) \phi_{my}(y) \eta_{nm}(t) \quad (7)$$

The shape functions are as of a flexible Euler-Bernoulli beam verifying the same boundary conditions as a pinned-free beam in x-direction (named bending), and to free-free beam in y-direction (named here as torsion), according Fig. (6). In this way, the mode shapes to bending (n = 1, 2, 3, ...) are:

$$\phi_{nx}(x) = A_{nx} \left\{ \cos \beta_{nx} ((a-x)/a) + \cosh \beta_{nx} ((a-x)/a) - \frac{\cosh \beta_{nx} a - \cos \beta_{nx} a}{\sinh \beta_{nx} a - \sin \beta_{nx} a} \left[(\sin \beta_{nx} ((a-x)/a) + \sinh \beta_{nx} ((a-x)/a)) \right] \right\} \quad (8)$$

with the following boundary conditions:

$$x = 0: \phi_{nx}(0) = 0 \text{ and } \phi_{nx}''(0) = 0; \quad x = a: \phi_{nx}''(a) = 0 \text{ and } \phi_{nx}'''(a) = 0 \quad (9.a,b)$$

and satisfying the orthogonality relations:
$$\int_0^a \phi_{nx} \phi_{px} dx = a \delta_{np} \quad (10)$$

The torsional motion is described by (m = 1): $\phi_{1y}(y) = A_{1y}$ and (m = 2): $\phi_{2y}(y) = A_{2y} \left(y - \frac{b}{2} \right)$

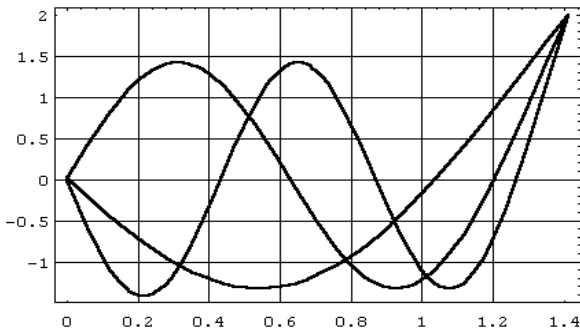
and the mode shapes in torsion, (m = 3, 4, 5, ...) are given by:

$$\phi_{my}(y) = A_{my} \left[\frac{\cos \beta_{my} b - \cosh \beta_{my} b}{\sin \beta_{my} b - \sinh \beta_{my} b} (\sin \beta_{my} y + \sinh \beta_{my} y) - (\cos \beta_{my} y + \cosh \beta_{my} y) \right] \quad (11)$$

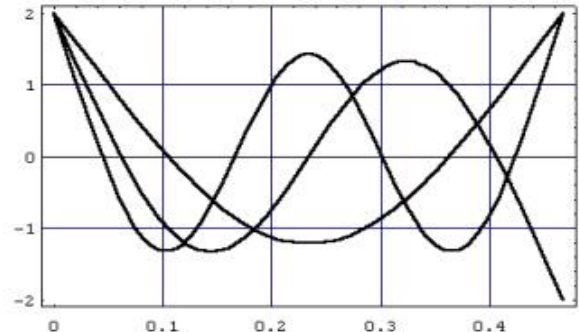
with the boundary conditions $\phi_{my}''(0) = 0; \phi_{my}'''(0) = 0;$

$$\phi_{my}''(b) = 0; \phi_{my}'''(b) = 0 \quad (12)$$

and the following orthogonality relations
$$\int_0^b \phi_{my} \phi_{qy} dy = b \delta_{mq} \quad (13)$$



(a)



(b)

Figure 6. (a) Plot of the shape functions of bending (n = 1, 2, 3) and (b) Plot of shape functions of torsion (m = 3, 4, 5)

Substituting the assumed modes, described by Eq. (8) and Eq. (11), in the governing equations of motion of the plate, Eq. (6b), one arrives at the matrix equation describing the free vibration of the plate system

$$\underline{\underline{M}}\ddot{\underline{\eta}} + \underline{\underline{K}}\underline{\eta} = \underline{0} \quad (14)$$

where the mass and stiffness matrices are:

$$\underline{\underline{M}}_{ij} = \int_0^a \int_0^b \phi_{px} \phi_{qy} m_j dx dy \quad \underline{\underline{K}}_{ij} = \int_0^a \int_0^b \phi_{px} \phi_{qy} k_j dx dy$$

with $m_j = m\phi_{nx} \phi_{my}$

$$k_j = D(\phi_{nx}^{iv} \phi_{my} + 2\phi_{nx}^{ii} \phi_{my}^{ii} + \phi_{nx} \phi_{my}^{iv}), \quad j = R.(m-1) + n \quad (15.a,b)$$

The natural motion of the system is described by the natural modes obtained solving the eigenvalue equation $(\underline{\underline{M}}^{-1} \underline{\underline{K}} - \omega^2 \underline{I}) \underline{\eta} = \underline{0}$. Substituting the physical parameters of the plant, one arrives at the following theoretical estimates for the first mode frequencies of the system, arranged in descending order and expressed in [Hertz],

$$\{f_i; i = 1, 2, \dots, 7\} = [86,1; 73,5; 66,8; 56,8; 33,2; 15,9; 4,91] \quad (16)$$

3.1 BG Model of the Slewing Plate

In this section we propose a BG representation for the dynamics of the slewing plate supported by a central rotating rigid hub, shown in Fig. (5). Introducing in the equation of motion, Eq. (6b), a concentrated externally controlled moment $T(x, y, t) = T_0 \delta'(y)$ and a concentrated external efforts:

$$F(x, y, t) = F_1 \delta(x - x_1) \delta(y - y_1) + F_2 \delta(x - x_2) \delta(y - y_2) \quad (17)$$

and making use of the mode shapes (8) and (11), multiplying by $\phi_{px} \phi_{qy}$ and integrating over the area, we find the equations as follows bellow. The equation of motion considering just the translation in y-direction, i e, m=1, is given by:

$$m_{n1} \ddot{\eta}_{n1} + k_{n1}^T \eta_{n1} = b \phi_{nx}'(0) \tau + F_1 \int_0^a \phi_{nx} dx + F_2 \int_0^a \phi_{nx} dx \quad (18)$$

where the modal mass and stiffness coefficients are

$$m_{n1} = mab \quad k_{n1}^T = Db \int_0^a \phi_{nx}^{iv} \phi_{nx} dx$$

In rotation, (m = 2), the equation of motion is described by:

$$J_g \ddot{\eta}_{n2} + \frac{J_g D}{ma} \int_0^a \phi_{nx}^{iv} \phi_{nx} dx \eta_{n2} = F_1 \frac{2\sqrt{3}}{b} \left(y_1 - \frac{b}{2} \right) \int_0^a \phi_{nx} dx + F_2 \frac{2\sqrt{3}}{b} \left(y_2 - \frac{b}{2} \right) \int_0^a \phi_{nx} dx \quad (19)$$

The flexible modes (n = 1,2,3,...; m = 3,4,5...) are described by:

$$m_{nm} \ddot{\eta}_{nm} + k_{nm}^F \eta_{nm} = F_1 \phi_{qy}(y_1) \int_0^a \phi_{nx} dx + F_2 \phi_{qy}(y_2) \int_0^a \phi_{nx} dx + T_0 \phi_{nx}'(0) \int_0^b \phi_{my} dy \quad (20)$$

$$m_{nm} = mab; \quad k_{nm}^F = D \left[b \int_0^a \phi_{nx}^{iv} \phi_{nx} dx + 2 \int_0^a \phi_{nx}^{ii} \phi_{nx} dx \int_0^b \phi_{my}^{ii} \phi_{my} dy + a \int_0^b \phi_{my}^{iv} \phi_{my} dy \right] \quad (21)$$

The results described by Eqs. (18), (19) and (20) can be described in the BG language as shown in Fig. (7).

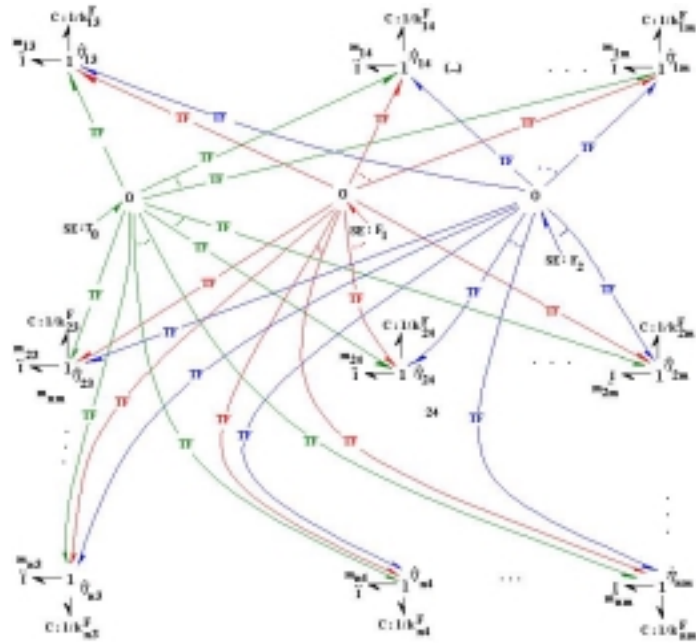


Figure 7. Bond-Graphs representation of the flexible plate

The BG description of the slewing link can now be coupled to the low-order equivalent system (LOES) for the hydraulic actuation system as previously described. The complete representation of the slewing flexible plate actuated by a servo hydraulic system is shown in Fig. (8).

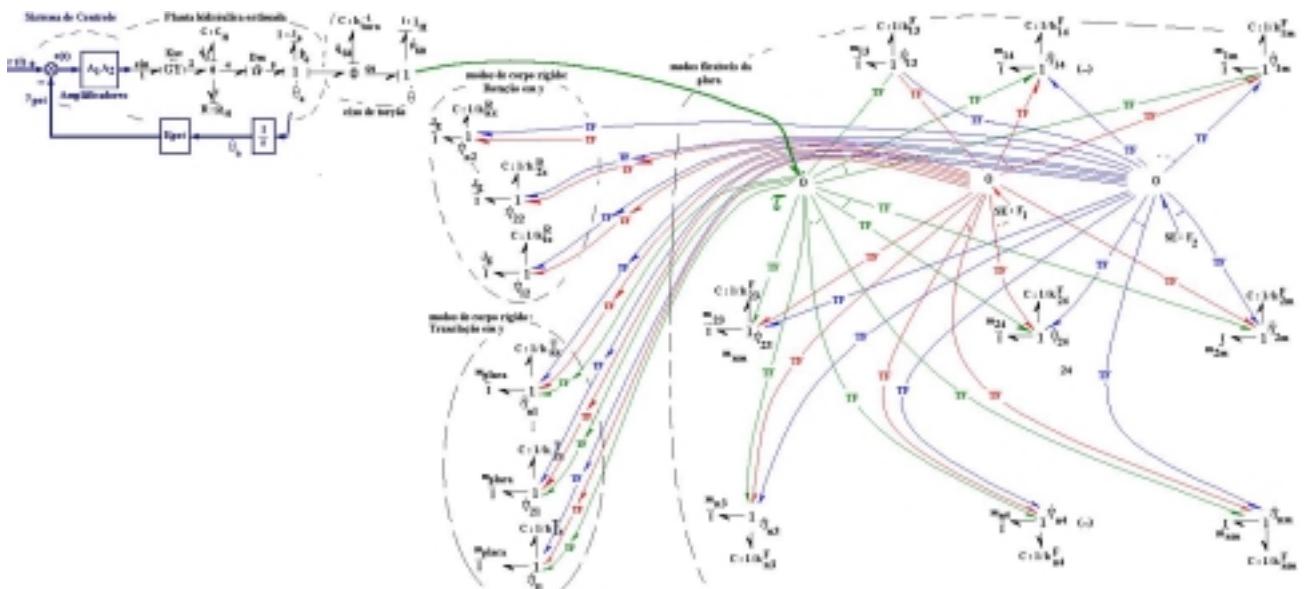


Figure 8. BG of the Control System of a Flexible Structure with Hydraulic Actuation

The colored lines depict graphically the influence of the control torque at the hub and the coupling forces and moments between the various flexible modes of the system. This is a unique way to visualize a complex dynamic system that has rigid body modes coupled to flexural and torsional energy in the system, besides the low order graphical description of the servo-actuation system.

4. BOND GRAPH SIMULATIONS

Computational simulations were realized with the aid of a special Computer Aided Modeling Program with Graphical Bond Graph input (CAMP-G). The BG model used in the simulation is shown in Fig. (9a). In this model we take $F_1 = F_2 = 0$. The simulation results can be validated by comparing the computed frequency response functions (FRF), calculated by taking the response of an accelerometer fixed at the free edge of the plate at, $x=a$ and $y=b/2$. The computed FRF, $[W/R](j\omega)$, is shown in Fig. (9b), where the output is computed as:

$$w\left(a, \frac{b}{2}, t\right) \cong z\left(a, \frac{b}{2}, t\right) = \sum_{n=1}^3 \sum_{m=1}^5 \phi_{nx}(a) \phi_{my}\left(\frac{b}{2}\right) \eta_{nm}(t) \quad (22)$$

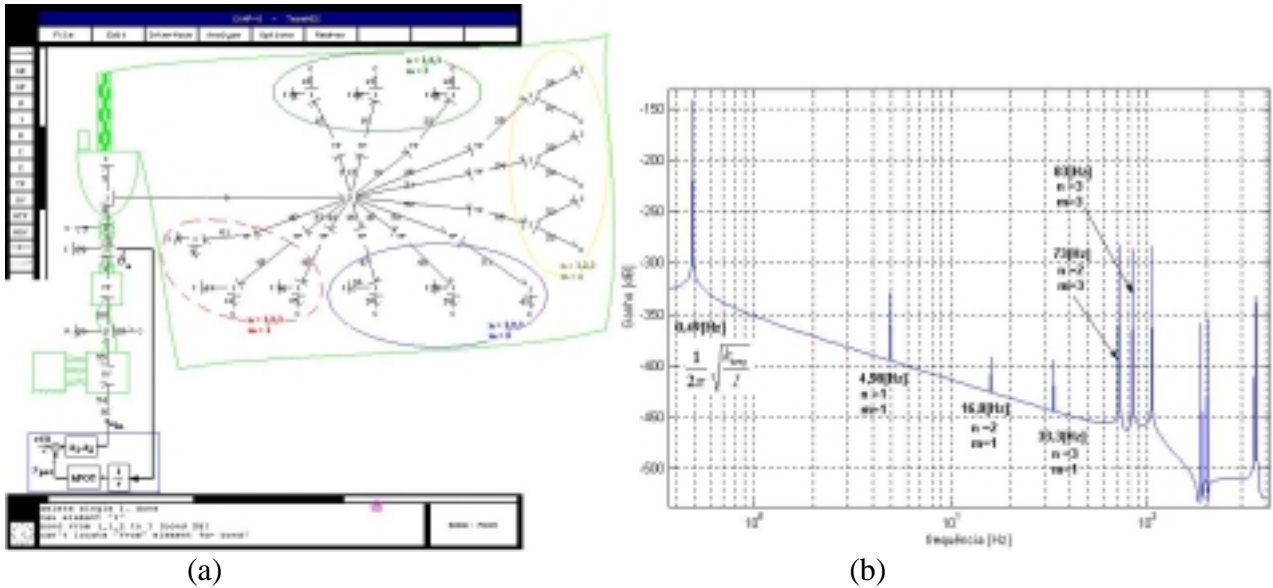


Figure 9. (a) Simulation of the system in CAMP-G and (b) Frequency Response Function (FRF) obtained with the linearized model described in the CAMP-G environment

4.1 Comparison with Experimental Results

In order to validate the computational BG simulation model, a comparison can be made between the computed FRF and the experimental FRF estimated by standard modal analysis. The experimentally determined FRFs are shown in Fig. (10). The plate was excited by an electrodynamic shaker, with the central hub locked in a fixed position.

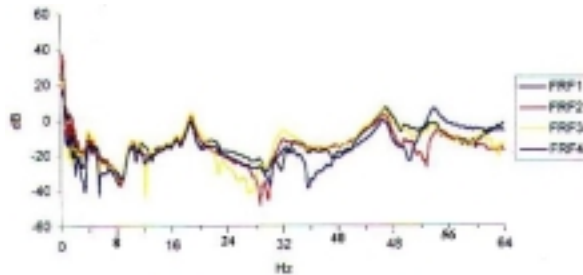


Figure 10. Experimental FRFs of the fixed plate, accelerometers 1, 2, 3 and 4

Figure (10) shows the FRFs obtained with four different accelerometers, distributed on the plate surface, according Fig. (5a). The natural modes of the flexible appendage estimated by the resonance peaks of the experimental transfer functions can be compared with the analytical

frequencies given in Eq. (16), and with the frequencies of the resonance peaks of the FRF shown in Fig. (9b). This comparison is summarized in Tab. (1) as follows.

Table 1. Resonance of frequencies of the flexible system, [Hz]

Analytical frequencies	Frequencies from the FRF of Fig. (9b)	Frequencies estimated from the FRF shown in Fig. (10)
4,41	4,98	5,0
15,9	16,0	19,0
33,2	33,3	33,0
66,8	66,0	*
73,5	73	*
86,1	84	*

* Out of band analysis

5. CONCLUSIONS

This work presents a proposal for a BG model representation of a slewing flexible plate controlled by a hydraulic servo control system. The BG model reproduced the principal characteristics of this complex dynamic system, with the advantage of providing a direct visualization of the principal dynamic effects and its coupling characteristics. The numerical results of the BG simulation showed that the model is consistent and robust. The comparison between the BG derived eigenvalues with the resonant peaks of the experimentally determined FRF show again the good agreement between model results and experimental observations.

The BG derived analytical frequencies 4,9; 16,9 and 33,2 [Hz] can be associated with the experimentally observed flexible modes $(n, m) = (1,1)$, $(2,1)$ and $(3,1)$, respectively. Other analytical frequencies at 73,5 and 86,1[Hz] are coherent with the modes $(n,m) = (2,3)$ and $(3,3)$, respectively. The frequency at 66,0 [Hz] is associated with flexible mode $(n,m) = (1,3)$.

6. REFERENCES

- CUNHA, W. P. **Sistema para medições de propriedades de massa**. 1993. 120 f. Dissertação (Mestrado em Engenharia Mecânica) - Instituto Tecnológico de Aeronáutica, São José dos Campos.
- FARIBORZI, F. et al. Development of mathematical model of a plate for active vibration suppression. **Journal of Vibration and Control**, v. 5, p. 175-194, 1999.
- GERADIN, M., RIXEN, D. **Mechanical vibrations: theory and application to structural dynamics**. Paris: Masson, 1994.
- GRANDA, J. J. **New developments in Bond Graph modeling software tools: the computer aided modeling program CAMP-G and MATLAB**. In: IEEE INTERNATIONAL CONFERENCE ON SYSTEMS, Man, And Cybernetics, Hyatt Orlando, Florida, USA, oct., 12-15 1997.
- KARNOPP, D. C.; MARGOLIS D. L.; ROSENBERG, R. C. **System dynamics: a unified approach**. New York, NY.: Wiley-Interscience Publication, 1990.
- MEIROVITCH, L. **Analytical methods in vibration**. New York, NY.: The Mcmillan Company, 1967. 555 p.
- MERRITT, H. E. **Hydraulic control systems**. New York, NY.: John Wiley & Sons, 1967. 358 p.
- SZILARD, R. **Theory and analysis of plates – classical and numerical methods**. New Jersey: Prentice Hall, 1974.